DALTON
FULL PAPER

Selenium and tellurium derivatives of a monocarbon platinacarbaborane complex†

Stewart A. Batten,[a] John C. Jeffery,[a] Leigh H. Rees,[a] Martin D. Rudd[b] and F. Gordon A. Stone*[,b]

[a] *School of Chemistry, The University, Bristol, UK BS8 1TS*
[b] *Department of Chemistry, Baylor University, Waco, TX 76798-7348, USA*

The reaction between Na[Pt(PEt$_3$)$_2$(η^5-7-CB$_{10}$H$_{11}$)] **1** and PhSeCl in thf (tetrahydrofuran) afforded a mixture containing the isomeric species [Pt(SePh)(PEt$_3$)(η^5-*n*-SePh-7-CB$_{10}$H$_{10}$)] (*n* = 8 **2a** or 9 **2b**) and the compound [Pt(SePh)(PEt$_3$){η^5-8-O(CH$_2$)$_4$Cl-7-CB$_{10}$H$_{10}$}] **3**. The molecular structures of complexes **2a** and **3** were established by X-ray crystallography. Both molecules have Pt(SePh)(PEt$_3$) groups with the platinum atoms pentahapto co-ordinated by *nido*-7-CB$_{10}$ cage frameworks. In **2a** the cage substituted SePh group is attached to the boron atom in the α site with respect to the carbon in the $\overline{\mathrm{C}B\mathrm{BBB}}$ ring ligating the platinum and this is true also of the O(CH$_2$)$_4$Cl substituent in **3**. The isomers **2** are also formed when PhSeSePh is used instead of PhSeCl. Treatment of the salt **1** with PhTeI in thf yielded a mixture of [Pt(PEt$_3$)$_2${η^5-9-Te(Ph)CH$_2$Cl-7-CB$_{10}$H$_{10}$}] **4** and [Pt$_2$(TePh)(μ-TePh)$_2$(PEt$_3$)$_2$(η^5-2-CB$_{10}$H$_{11}$)] **5**. Single-crystal X-ray diffraction studies were employed to establish the formulations and molecular structures of both molecules. Compound **4** is a charge-compensated platinacarbaborane with a Pt(PEt$_3$)$_2$ group and with the *nido*-7-CB$_{10}$ framework carrying a Te(Ph)CH$_2$Cl moiety at the boron vertex situated in the β site with respect to the carbon in the $\overline{\mathrm{CB}B\mathrm{BB}}$ ring ligating the platinum. Complex **5** is a diplatinum species in which Pt(TePh)(PEt$_3$) and Pt(PEt$_3$)(η^5-2-CB$_{10}$H$_{11}$) units are bridged by two TePh groups. The X-ray study revealed that in forming compound **5** from the reagent **1** the *nido*-7-CB$_{10}$H$_{11}$ cage system has undergone an unusual polytopal rearrangement to a *nido*-2-CB$_{10}$H$_{11}$ framework.

As part of studies[1] directed towards extending the range of monocarbon metallacarbaboranes with icosahedral frameworks, the salt Na[Pt(PEt$_3$)$_2$(η^5-7-CB$_{10}$H$_{11}$)] **1** has been prepared and used to obtain a variety of new products, including the heterodinuclear metal compounds [PtM(PEt$_3$)$_2$L(η^5-7-CB$_{10}$H$_{11}$)] (M = Cu or Au, L = PPh$_3$; M = Hg, L = Ph).[1a] The latter were prepared by treating the reagent **1** with the chloro complexes [MCl(PPh$_3$)] (M = Cu or Au) and [HgCl(Ph)], respectively. Formation of these dimetal species suggested that a similar reaction between the platinum species **1** and the compounds PhSeCl or PhTeI should yield as products the complexes [Pt(EPh)(PEt$_3$)$_2$(η^5-7-CB$_{10}$H$_{11}$)] (E = Se or Te). These compounds would be of interest since as far as we are aware platinacarbaborane cage complexes in which the platinum vertex is exopolyhedrally bonded to selenium or tellurium are not known. Moreover, the desired products might be potentially useful as reagents for further syntheses by virtue of the donor properties of lone pairs associated with the Se or Te atoms. However, instead of obtaining the anticipated complexes [Pt(EPh)(PEt$_3$)$_2$(η^5-7-CB$_{10}$H$_{11}$)] (E = Se or Te), mixtures of products were isolated as a consequence of reactions occurring at BH groups of the $\overline{\mathrm{CBBBB}}$ face of the *nido*-7-CB$_{10}$H$_{11}$ cage ligating the platinum.

Results and discussion

Addition of the reagent **1** in thf (tetrahydrofuran) to a solution of PhSeCl in the same solvent afforded at ambient temperatures a mixture of products which were separated by column chromatography. Two isomeric species [Pt(SePh)(PEt$_3$)(η^5-*n*-SePh-7-CB$_{10}$H$_{10}$)] (*n* = 8 **2a** or 9 **2b**) were obtained, but also formed were the compounds [Pt(SePh)(PEt$_3$){η^5-8-O(CH$_2$)$_4$Cl-7-CB$_{10}$H$_{10}$}] **3** and [Pt(SePh)$_2$(PEt$_3$)$_2$]. These complexes were characterised by microanalysis and NMR spectroscopy (Table 1), and for **2a** and **3** also by single-crystal X-ray diffraction studies. A mixture of the isomers **2** was also isolated when PhSeSePh was used instead of PhSeCl.

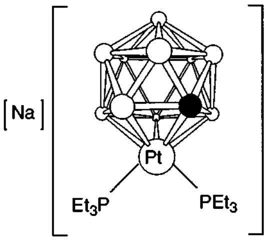

1

The molecule **2a** is shown in Fig. 1 and selected bond distances and angles are listed in Table 2. It is immediately apparent that there are two SePh groups one of which is attached to the platinum atom and the other exopolyhedrally to a boron atom of the *nido*-7-CB$_{10}$H$_{10}$ fragment. Moreover, B(2), the atom of the carbaborane group to which the SePh group is attached, is located in an α site with respect to the carbon in the $\overline{\mathrm{C}B\mathrm{BBB}}$ ring ligating the platinum. The Se(2)–B(2) distance [1.984(9) Å] in **2a** is somewhat shorter than those [2.016(15) and 2.023(16) Å] in the salt [NEt$_4$]$_2$[Se$_3$B$_{11}$H$_9$], a disubstituted derivative of [*closo*-B$_{11}$H$_{11}$]$^{2-}$ in which an Se$_3$ chain bridges two boron atoms.[2]

The Pt–Se(1) separation [2.4438(8) Å] lies within the range [2.376(2)–2.590(7) Å] observed in various complexes containing Pt–Se bonds.[3] Interestingly, however, the Pt–Se(1) connectivity is shorter than those [2.676(1) Å] in the complexes [Pt(PR$_3$)$_2$(η^5-7-SeB$_{10}$H$_{10}$)] (R = Et or Ph) where the selenium atom is a vertex in a *closo*-cage system.[4] Of interest is whether the Se(1)Ph group of **2a** formally contributes one electron to the valence shell of

---

† The complexes described in this paper have a platinum atom incorporated into a *closo*-1-carba-2-platinadodecaborane structure. However, to avoid a complicated nomenclature for the compounds reported, and to relate them to species with pentahapto-co-ordinated cyclopentadienyl ligands, following precedent (see ref. 1) we treat the cages as *nido*-11-vertex ligands with numbering as for an icosahedron from which the twelfth vertex has been removed.

Table 1 Hydrogen-1, carbon-13, boron-11 and phosphorus-31 NMR data[a]

Compound	^{1}H (δ)	^{13}C (δ)[b]	^{11}B (δ)[c]	^{31}P (δ)[d]
2a	1.25 [d of t, 9 H, Me, *J*(PH) 16, *J*(HH) 8], 2.23 [d of q, 6 H, CH_2, *J*(PH) 15, *J*(HH) 8], 3.50 (s br, 1 H, cage CH), 6.60–7.57 (m, 10 H, Ph)	137.2–128.3 (m, Ph), 49.0 (br, cage CH), 18.5 [d, P*C*H_2Me, *J*(PC) 15], 8.3 [d, PCH_2*Me*, *J*(PC) 8]	21.7 (1 B, BSe), 19.3 (1 B), 8.0 (1 B), 4.7 (1 B), 3.0 (1 B), −5.2 (1 B), −8.8 (1 B), −10.3 (1 B), −14.1 (1 B), −15.2 (1 B)	27.8 [*J*(PtP) 3283]
2b[e]	1.26 [d of t, 9 H, Me, *J*(PH) 16, *J*(HH) 8], 2.25 [d of q, 6 H, CH_2, *J*(PH) 15, *J*(HH) 8], 3.53 (s br, 1 H, cage CH), 6.60–7.57 (m, 10 H, Ph)		23.5 (1 B, BSe), 20.1 (1 B), 7.1 (1 B), 3.2 (1 B), −1.0 (1 B), −5.3 (1 B), −8.3 (1 B), −10.5 (1 B), −17.4 (2 B)	26.5 [*J*(PtP) 3469]
3	1.24 [d of t, 9 H, Me, *J*(PH) 16, *J*(HH) 8], 1.74–1.91 (m, 4 H, OCH_2 and CH_2Cl), 2.50 [d of t, 6 H, P*C*H_2Me, *J*(PH) 16, *J*(HH) 8], 3.40–3.72 (m, 4 H, $CH_2CH_2CH_2CH_2$), 7.21–7.50 (m, 5 H, Ph)	137.0–128.5 (m, Ph), 69.6 (s, OCH_2), 65.3 (br, cage CH), 45.2 (CH_2Cl), 29.6 (CH_2), 28.6 (CH_2), 17.4 [d, P*C*H_2Me, *J*(PC) 37], 7.8 [d, PCH_2*Me*, *J*(PC) 8]	22.2 (1 B, $BOCH_2$), 19.2 (1 B), 13.3 (1 B), 6.7 (2 B), −8.5 (2 B), −10.5 (1 B), −11.9 (1 B), −20.8 (1 B)	35.4 [*J*(PtP) 3147]
4	0.70 [d of t, 9 H, Me, *J*(PH) 14, *J*(HH) 8], 1.08 [d of t, 9 H, Me, *J*(PH) 15, *J*(HH) 7], 1.86 [d of q, 6 H, CH_2, *J*(PH) 15, *J*(HH) 8], 2.09 (m, 6 H, CH_2), 2.57 (s, 1 H, cage CH), 4.46, 4.52 [AB, 2 H, CH_2Cl, *J*(AB) 5], 7.43–7.84 (m, 5 H, Ph)	136.6–130.3 (m, Ph), 50.2 (br, cage CH), 32.8 (CH_2Cl), 18.8 (m, P*C*H_2Me), 8.5 (m, PCH_2-*Me*)	−4.7 (1 B, BTe), −9.6 (2 B), −20.2 (5 B), −25.1 (2 B)	−0.23 [*J*(PtP) 3513], 0.85 [*J*(PtP) 3190]
5	0.96 (m, 18 H, Me), 1.54–2.24 (m, 12 H, CH_2), 2.66 (s br, 1 H, cage CH), 6.77–7.90 (m, 15 H, Ph)	142.4–127.6 (m, Ph), 45.5 (br, cage CH), 18.1 (m, P*C*H_2Me), 9.5 (m, PCH_2*Me*)	2.0 (3 B), −3.5 (3 B), −13.9 (4 B)	1.23 [*J*(PtP) 2997], 2.11 [*J*(PtP) 2988]

[a] Chemical shifts in ppm, coupling constants in Hz, measurements in CD_2Cl_2 at room temperature. [b] Hydrogen-1 decoupled, chemical shifts are positive to high frequency of $SiMe_4$. [c] Hydrogen-1 decoupled, chemical shifts are positive to high frequency of $BF_3{\cdot}Et_2O$ (external). Assignments for BX (X = Se, Te or OCH_2) groups made from the observation of resonance as a singlet peak in a fully coupled ^{11}B spectrum. [d] Hydrogen-1 decoupled, chemical shifts are positive to high frequency of 85% H_3PO_4 (external). [e] The ^{13}C-{^{1}H} spectrum was too weak to give meaningful data.

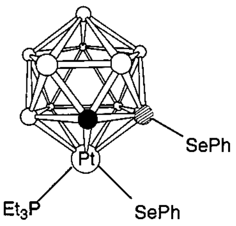

2a

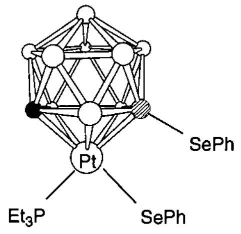

2b

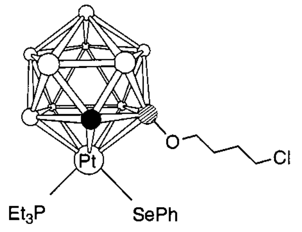

3

○BH ▨B ●CH

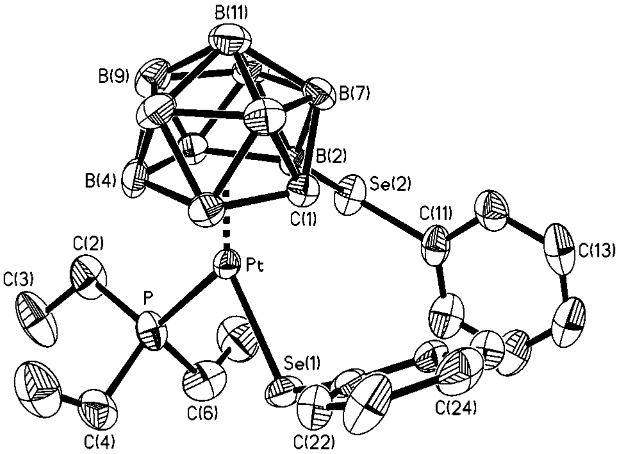

Fig. 1 Molecular structure of [Pt(SePh)(PEt_3)(η^5-8-SePh-7-$CB_{10}H_{10}$)] **2a** showing the atom labelling scheme. Ellipsoids are drawn at the 40% probability level and hydrogen atoms are omitted for clarity

platinum or three if a lone pair on the selenium π bonds to the metal center. The angles Pt–Se(1)–C(21) [106.2(2)°] and B(2)–Se(2)–C(11) [105.4(3)°] are very similar, and of a magnitude suggesting that the selenium atoms in the two sites are both sp^3 hybridised. It is thus reasonable to suppose that Pt–Se(1) is a σ bond involving an electron pair, and hence with the PEt_3 and η^5-8-SePh-7-$CB_{10}H_{10}$ ligands contributing two and three electrons, respectively, overall the platinum atom has 16 electrons in its valence shell. The Pt–P distance [2.330(2) Å] is similar to that in [PtAu(PEt_3)$_2$(PPh_3)(η^5-7-$CB_{10}H_{11}$)] [2.3487(14) Å].[1a] The average found for the many complexes with Pt–PEt_3 bonds studied by X-ray diffraction is 2.296 Å, though these separations vary slightly with the co-ordination number of the platinum.[5]

The NMR data (Table 1) for complex **2a** are in accord with the structure established by X-ray diffraction. The ^{1}H NMR spectrum reveals a diagnostic broad peak for the cage CH group at δ 3.50 while a characteristic resonance for this group is also seen in the ^{13}C-{^{1}H} spectrum at δ 49.0.[1] In the ^{11}B-{^{1}H} NMR spectrum there are ten signals in accord with the asymmetry of the *nido*-8-SePh-7-$CB_{10}H_{10}$ fragment. The resonance in this spectrum at δ 21.7 may be ascribed to the *B*SePh nucleus as it remained a singlet in a fully coupled ^{11}B spectrum, whereas the other peaks became doublets [*J*(BH) > 100 Hz]. The ^{31}P-{^{1}H} NMR spectrum was as expected, a singlet (δ 27.8) with ^{195}Pt satellite peaks.

The microanalytical data for complex **2b** established that it

Table 2 Selected internuclear distances (Å) and angles (°) for [Pt(SePh)(PEt$_3$)(η^5-8-SePh-7-CB$_{10}$H$_{10}$)] **2a** with estimated standard deviations (e.s.d.s) in parentheses

Pt–B(2)	2.178(8)	Pt–B(5)	2.195(9)	Pt–C(1)	2.230(7)	Pt–B(4)	2.231(9)
Pt–B(3)	2.278(8)	Pt–P	2.330(2)	Pt–Se(1)	2.4438(8)	Se(1)–C(21)	1.934(8)
Se(2)–C(11)	1.936(8)	Se(2)–B(2)	1.984(9)	C(1)–B(2)	1.732(11)	C(1)–B(5)	1.766(11)
B(2)–B(3)	1.876(11)	B(3)–B(4)	1.797(12)	C(11)–C(16)	1.385(12)	C(11)–C(12)	1.428(11)
C(12)–C(13)	1.345(11)	C(13)–C(14)	1.411(13)	C(14)–C(15)	1.347(12)	C(15)–C(16)	1.403(12)
C(21)–C(22)	1.373(11)	C(21)–C(26)	1.398(10)	C(22)–C(23)	1.368(11)	C(23)–C(24)	1.406(11)
C(24)–C(25)	1.376(11)	C(25)–C(26)	1.381(11)				
B(2)–Pt–B(5)	82.2(3)	B(2)–Pt–C(1)	46.2(3)	B(5)–Pt–C(1)	47.0(3)		
B(2)–Pt–B(4)	82.4(3)	B(5)–Pt–B(4)	50.8(3)	C(1)–Pt–B(4)	81.9(3)		
B(2)–Pt–B(3)	49.7(3)	B(5)–Pt–B(3)	84.3(3)	C(1)–Pt–B(3)	82.0(3)		
B(4)–Pt–B(3)	47.0(3)	B(2)–Pt–P	132.8(2)	B(5)–Pt–P	131.7(2)		
C(1)–Pt–P	177.6(2)	B(4)–Pt–P	95.8(3)	B(3)–Pt–P	95.8(2)		
B(2)–Pt–Se(1)	123.7(2)	B(5)–Pt–Se(1)	101.5(2)	C(1)–Pt–Se(1)	96.8(2)		
B(4)–Pt–Se(1)	142.0(2)	B(3)–Pt–Se(1)	170.9(2)	P–Pt–Se(1)	85.49(6)		
C(21)–Se(1)–Pt	106.2(2)	C(11)–Se(2)–B(2)	105.4(3)	C(1)–B(2)–Se(2)	127.8(5)		
B(8)–B(2)–Se(2)	121.3(6)	B(7)–B(2)–Se(2)	129.6(5)	B(3)–B(2)–Se(2)	111.7(5)		
Se(2)–B(2)–Pt	100.3(4)	C(16)–C(11)–Se(2)	118.1(7)	C(12)–C(11)–Se(2)	121.6(7)		
C(22)–C(21)–Se(1)	120.2(6)	C(26)–C(21)–Se(1)	119.5(6)				

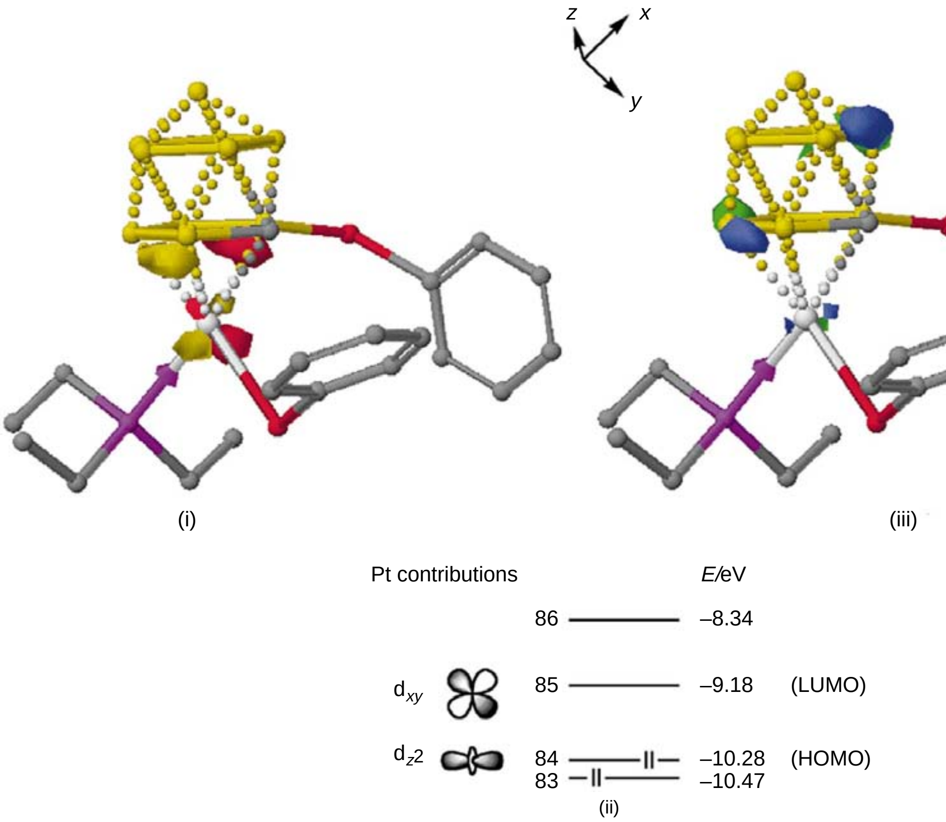

Fig. 2 Extended Hückel MO calculations for complex **2a**: (i) LUMO, (ii) Frontier energy levels, (iii) HOMO. Key: boron, yellow; carbon, grey; selenium, red; phosphorus, pink; platinum, silver

had the same elemental composition as **2a**. Moreover, the ^{1}H, ^{31}P-{^{1}H}, and ^{11}B-{^{1}H} NMR data for the two species are very similar (Table 1). On the basis of earlier studies[1] we identify **2b** as [Pt(SePh)(PEt$_3$)(η^5-9-SePh-7-CB$_{10}$H$_{10}$)] the isomer in which the SePh cage substituent is attached to a boron atom in the β site in the CB*B*BB ring co-ordinated to the platinum atom.

The presence of stable 16e$^-$ platinum(IV) centers in the complexes **2** is somewhat unusual and prompted us to examine the frontier orbitals of **2a**. Using the atomic coordinates generated by the crystal structure determination, an extended Hückel MO calculation[6] was carried out. The LUMO [Fig. 2(i)] is a π-symmetry orbital which primarily consists of a platinum d$_{xy}$ atomic orbital in antibonding combination with carbaborane cage atomic orbitals in the CBBBB co-ordinating face. It lies some 1.1 eV (1 eV ≈ 1.60 × 10^{-19} J) higher in energy [Fig. 2(ii)] above the HOMO [Fig. 2(iii)], which comprises a significant contribution from the platinum d$_{z^2}$ orbital, the latter being in bonding combination with cage atomic orbitals. Thus **2a** does not seem particularly electronically susceptible to attack by the lone pair of, say, a second PEt$_3$ ligand. This was indeed observed to be the case as attempts to add 1 equivalent of PEt$_3$ to the complexes **2** did not succeed. Treatment of **2a** with the rod-like ligand CNBu^t also failed to afford an 18-electron complex [Pt(SePh)(CNBu^t)(PEt$_3$)(η^5-8-SePh-7-CB$_{10}$H$_{10}$)]. Furthermore, examination of the space-filling diagram of **2a** (Fig. 3) reveals that approach of an extra co-ordinating ligand would be severely sterically hindered; there is little room to accommodate further groups around the platinum, even when the cage-bound SePh has its phenyl group oriented away from the metal center.

As mentioned above, there was no evidence from the X-ray diffraction study that selenium lone pairs elevated the electron count at the platinum, and this is supported by the absence of any contribution of these lone pair atomic orbitals to the frontier HOMO region. The question arises as to why the complexes **2** do not increase their co-ordination number, while the complexes [PtM(PEt$_3$)$_2$L(η^5-7-CB$_{10}$H$_{11}$)] (M = Cu or Au, L = PPh$_3$; M = Hg, L = Ph)[1a] do achieve the expected 18e$^-$ count by co-ordination of two PEt$_3$ ligands rather than one. The problem would primarily appear to be one of a steric nature, for it is qualitatively intuitive that the Tolman cone angle,[7] θ_T, of the bent SePh group far exceeds that of the linear ML units in the complexes [PtM(PEt$_3$)$_2$L(η^5-7-CB$_{10}$H$_{11}$)] (M = Cu or Au, L = PPh$_3$; M = Hg, L = Ph).

A complicated series of reaction steps is evidently responsible for replacement of the H atom of a BH moiety in the reagent **1** by an SePh group in order to afford the isomers **2**. The pathway by which this occurs is obscure at the present time and any proposal is necessarily speculative. One possibility for the formation of **2a** (Scheme 1) is that the compound [Pt(SePh)(PEt$_3$)(η^5-7-CB$_{10}$H$_{11}$)] **A** is initially formed by nucleophilic attack of [Pt(PEt$_3$)$_2$(η^5-7-CB$_{10}$H$_{11}$)]$^-$ on PhSeCl or PhSeSePh with concomitant dissociation of phosphine. The loss of phosphine at this stage would be expected on the basis of the above discussion. The species **A** could in turn afford the zwitterionic molecule [Pt(PEt$_3$)$_2${η^5-8-Se(H)Ph-7-CB$_{10}$H$_{10}$}] **B** by migratory insertion of SePh into the B$_\alpha$–H bond of the nearby $\overline{\mathrm{CBBBB}}$ ring accompanied by reco-ordination of the phosphine to give an 18e$^-$ platinum center. Insertion of metal bonded alkylidene groups into adjacent B–H bonds in icosahedral metallacarbaboranes is well documented.[8] Deprotonation of the boron-bound Se(H)Ph group in **B** by traces of dissociated phosphine or X$^-$ (X = Cl$^-$ or SePh$^-$) would give the anionic reagent [Pt(PEt$_3$)$_2$(η^5-8-SePh-7-CB$_{10}$H$_{10}$)]$^-$ **C**, which could react further with PhSeX to give the complex **2a**. This mechanism would also account for the formation of **2b** by a route with intermediates similar to **B** and **C**, but with the selenium fragment bound to a β-boron atom in the $\overline{\mathrm{CB}B\mathrm{BB}}$ face of the cage.

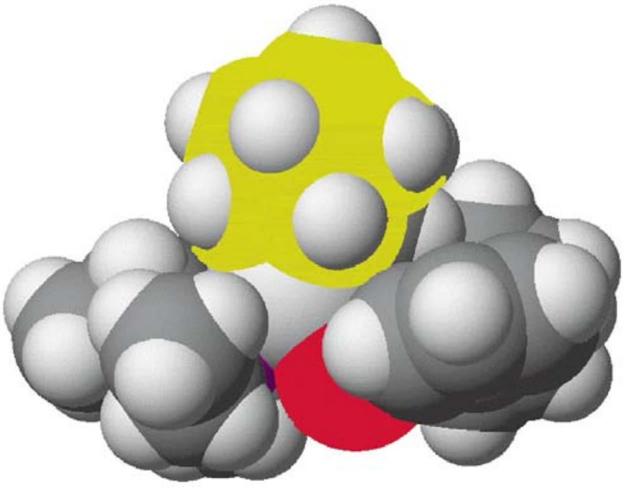

Fig. 3 Space-filling diagram of the molecule **2a** showing a lack of accessibility to the platinum. Colour key: as for Fig. 2

In the reaction between the salt **1** and PhSeCl, compound **3** was the product formed in highest yield (*ca.* 35%, compared with a combined yield of *ca.* 20–25% for the isomers **2** based on the platinum used). The nature of complex **3** only became evident after an X-ray diffraction study had been undertaken. The molecule is shown in Fig. 4 and selected internuclear distances and angles are given in Table 3. The platinum atom carries PEt$_3$ and SePh ligands as it does in complex **2a**. As might be expected the Pt–P [2.329(2) Å] and Pt–Se [2.4125(6) Å] bond lengths in complex **3** are very similar to those in compound **2a**. The carbaborane ligand in complex **3**, however, is a *nido*-7-CB$_{10}$H$_{10}$ cage fragment having an O(CH$_2$)$_4$Cl substituent attached to a boron atom in an α site in the $\overline{\mathrm{C}B\mathrm{BBB}}$ ring co-ordinated to the platinum. Thus complex **3** is established as having the formulation [Pt(SePh)(PEt$_3$){η^5-8-O(CH$_2$)$_4$Cl-7-CB$_{10}$H$_{10}$}]. We found no evidence for formation of an isomer [Pt(SePh)-

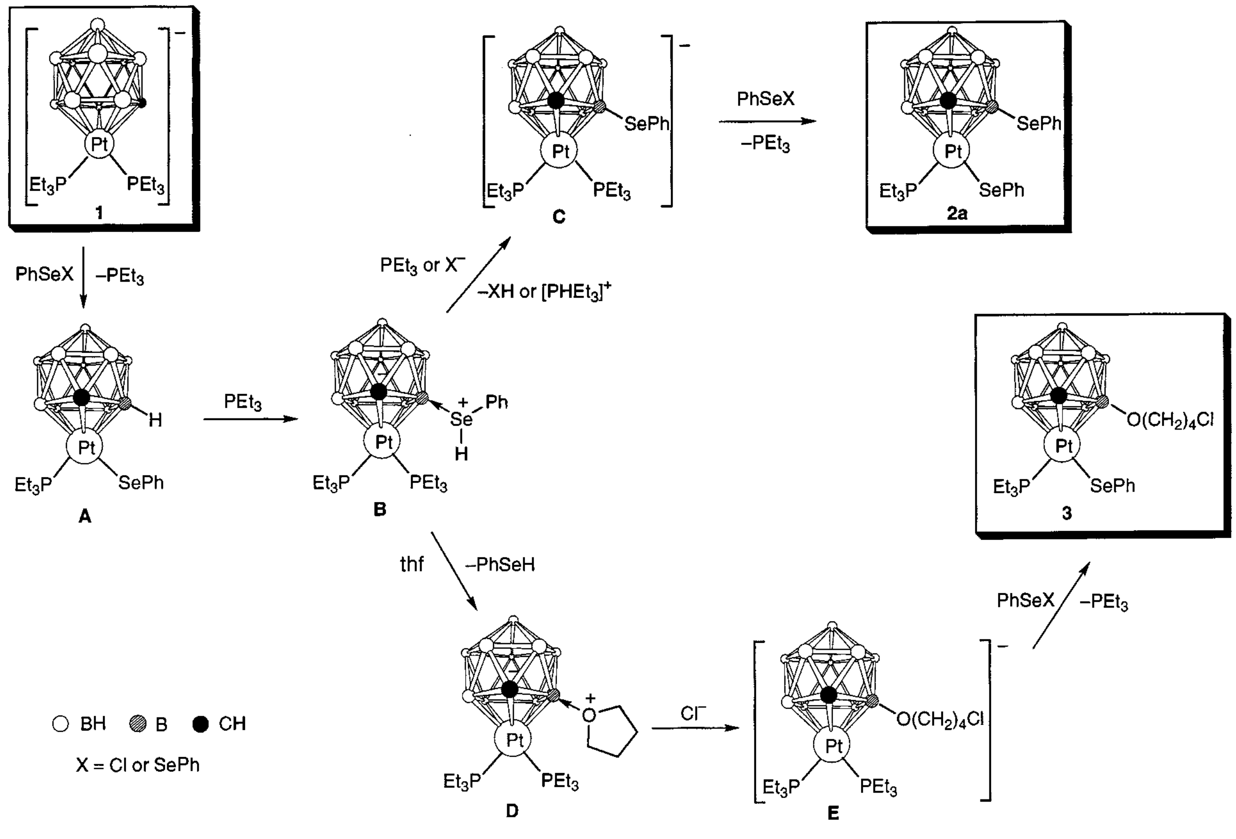

Scheme 1 Suggested pathways for the formation of complexes **2a** and **3**

Table 3 Selected internuclear distances (Å) and angles (°) for [Pt(SePh)(PEt$_3$){η^5-8-O(CH$_2$)$_4$Cl-7-CB$_{10}$H$_{10}$}] **3** with e.s.d.s in parentheses

Pt–B(5)	2.185(6)	Pt–B(2)	2.215(6)	Pt–B(3)	2.230(6)	Pt–B(4)	2.231(6)
Pt–C(1)	2.243(5)	Pt–P	2.329(2)	Pt–Se	2.4125(6)	Se–C(41)	1.924(5)
B(2)–O(51)	1.369(7)	B(2)–C(1)	1.754(8)	B(2)–B(8)	1.777(8)	B(2)–B(7)	1.810(9)
B(2)–B(3)	1.903(9)	P–C(31)	1.814(5)	P–C(11)	1.819(6)	P–C(21)	1.834(6)
Cl–C(55)	1.800(7)	C(1)–B(6)	1.688(8)	C(1)–B(7)	1.694(8)	C(1)–B(5)	1.745(8)
B(5)–B(10)	1.758(8)	B(5)–B(6)	1.783(8)	B(5)–B(4)	1.886(9)	B(4)–B(9)	1.768(8)
B(4)–B(10)	1.776(9)	B(4)–B(3)	1.778(9)	B(3)–B(9)	1.769(9)	B(3)–B(8)	1.781(9)
B(8)–B(9)	1.778(9)	B(8)–B(11)	1.784(9)	B(8)–B(7)	1.795(9)	B(7)–B(6)	1.734(9)
B(7)–B(11)	1.751(9)	B(6)–B(11)	1.774(9)	B(6)–B(10)	1.782(9)	B(10)–B(11)	1.783(9)
B(10)–B(9)	1.784(9)	B(9)–B(11)	1.763(9)				
B(5)–Pt–B(2)	82.4(2)	B(5)–Pt–B(3)	83.5(2)	B(2)–Pt–B(3)	50.7(2)		
B(5)–Pt–B(4)	50.5(2)	B(2)–Pt–B(4)	83.9(2)	B(3)–Pt–B(4)	47.0(2)		
B(5)–Pt–C(1)	46.4(2)	B(2)–Pt–C(1)	46.3(2)	B(3)–Pt–C(1)	81.5(2)		
B(4)–Pt–C(1)	81.7(2)	B(5)–Pt–P	127.9(2)	B(2)–Pt–P	136.0(2)		
B(3)–Pt–P	96.8(2)	B(4)–Pt–P	93.0(2)	C(1)–Pt–P	174.06(13)		
B(5)–Pt–Se	114.3(2)	B(2)–Pt–Se	112.7(2)	B(3)–Pt–Se	155.6(2)		
B(4)–Pt–Se	157.4(2)	C(1)–Pt–Se	98.50(13)	P–Pt–Se	85.39(4)		
C(41)–Se–Pt	107.9(2)	O(51)–B(2)–C(1)	120.6(4)	O(51)–B(2)–B(8)	126.4(5)		

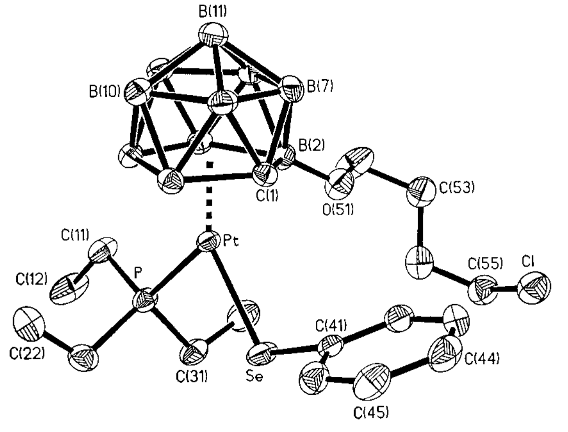

Fig. 4 Molecular structure of [Pt(SePh)(PEt$_3$){η^5-8-O(CH$_2$)$_4$Cl-7-CB$_{10}$H$_{10}$}] **3**. Details as in Fig. 1

(PEt$_3$){η^5-9-O(CH$_2$)$_4$Cl-7-CB$_{10}$H$_{10}$}] with the O(CH$_2$)$_4$Cl group attached to a β-boron in the $\overline{\mathrm{CB}\mathit{B}\mathrm{BB}}$ ring. It is noteworthy that isomer **2a** was isolated in about twice the amount of **2b** seemingly indicating a preference for substitution at α sites in the $\overline{\mathrm{CBBBB}}$ rings and it is possible that small amounts of [Pt(SePh)(PEt$_3$){η^5-9-O(CH$_2$)$_4$Cl-7-CB$_{10}$H$_{10}$}] were formed but lost in the work up procedures. However, we are currently assessing the preference for reactions at the BH$_\alpha$ or BH$_\beta$ sites and there are insufficient data available at the present time to draw any firm conclusions.

The O(CH$_2$)$_4$Cl group in compound **3** is reminiscent of the O(CH$_2$)$_4$F substituent attached to the cage in the molybdenum complex [NBu$^n_4$][Mo(CO)$_2$(η^3-C$_3$H$_5$){η^5-7,8-Me$_2$-10-O(CH$_2$)$_4$-F-7,8-C$_2$B$_9$H$_8$}]. The O(CH$_2$)$_4$F group in this molybdenum complex is formed by nucleophilic attack of F$^-$ ion on the three-co-ordinate oxygen atom of a thf molecule in the ylid complex [Mo(CO)$_2$(η^3-C$_3$H$_5$){η^5-7,8-Me$_2$-10-O(CH$_2$)$_4$-7,8-C$_2$-B$_9$H$_8$}].[9a] Similar ring opening of cyclic ethers attached to boron cage systems by nucleophiles has been reported for other systems.[9b,10] It thus seems certain that the O(CH$_2$)$_4$Cl group in **3** results from Cl$^-$ attack on a thf molecule co-ordinated to a cage boron atom. Chloride anion would be formed in the reaction of the salt **1** with PhSeCl and since thf is the solvent the necessary components for producing the O(CH$_2$)$_4$Cl fragment are present. Not unexpectedly **3** was not observed in the reaction between the reagent **1** and PhSeSePh since there is no source of Cl$^-$ under these conditions.

The pathway proposed above for the formation of the isomers **2** can be modified to accommodate the synthesis of complex **3** (Scheme 1). The boron-co-ordinated PhSeH molecule in the suggested zwitterionic intermediate **B** might readily be displaced by a thf molecule to give [Pt(PEt$_3$)$_2${η^5-8-O(CH$_2$)$_4$-7-CB$_{10}$H$_{10}$}] **D** in a process thermodynamically favoured on account of the strength of B–O bonds. A species **D** once formed would be expected[9] to react readily with Cl$^-$ to give [Pt(PEt$_3$)$_2$-{η^5-8-O(CH$_2$)$_4$Cl-7-CB$_{10}$H$_{10}$}]$^-$ **E**, and subsequently with PhSe-Cl to yield compound **3**.

The NMR data (Table 1) for complex **3** are in accord with the results of the X-ray diffraction study. In particular the ^{11}B-{^{1}H} NMR spectrum has a peak at δ 22.2 which may be ascribed to the *B*OCH$_2$ nucleus. It remained a singlet in a fully coupled ^{11}B spectrum and moreover the chemical shift may be compared with that observed (δ 20.1) for the *B*OCH$_2$ nucleus in [NBu$^n_4$]-[Mo(CO)$_2$(η^3-C$_3$H$_5$){η^5-7,8-Me$_2$-10-O(CH$_2$)$_4$F-7,8-C$_2$B$_9$H$_8$}].[9a] Other peaks in the NMR spectra of compound **3** are readily assigned.

The pathway by which [Pt(SePh)$_2$(PEt$_3$)$_2$] is formed in the reactions is very unclear. It may form from [PtCl$_2$(PEt$_3$)$_2$] and NaSePh. Some [PtCl$_2$(PEt$_3$)$_2$] might be present as a contaminant in the reagent **1** as it is a precursor of this salt,[1] while NaSePh could be generated at some point in the complicated reaction pathways.

Following investigation of reactions between the reagent **1** and the selenium compounds the study was continued with tellurium using PhTeI generated *in situ* by adding iodine to PhTeTePh.[11] The salt **1** and PhTeI in thf afforded two products, one yellow (**4**) and the other red (**5**), which were separable by column chromatography. Neither could be fully characterised solely by microanalysis and NMR spectroscopy so an X-ray crystallographic study was carried out on each.

Compound **4** proved to be the zwitterionic species [Pt(PEt$_3$)$_2$-{η^5-9-Te(Ph)CH$_2$Cl-7-CB$_{10}$H$_{10}$}]. Many such charge-compensated metallacarbaboranes are known.[9,12] The molecule **4** is shown in Fig. 5 and selected internuclear distances and angles are listed in Table 4. The platinum is ligated on one side by two PEt$_3$ groups. The two Pt–P bond distances average 2.313 Å and are very similar to those found in the molecules **2a** and **3**, and close to the average (2.288 Å) observed in several other platinum complexes having this ligand when the metal has a co-ordination number of four or five.[5] The other side of the platinum atom is pentahapto co-ordinated by a *nido*-9-Te(Ph)CH$_2$Cl-7-CB$_{10}$H$_{10}$ cage moiety. The Te(Ph)CH$_2$Cl fragment is attached to B(3) [B(3)–Te 2.215(6) Å] in the β site with respect to the carbon atom in the $\overline{\mathrm{CB}\mathit{B}\mathrm{BB}}$ ring. However, the formation of the group is inexplicable at the present time, although the CH$_2$Cl fragment must be derived from CH$_2$Cl$_2$. Since this solvent was only introduced during the work up procedures a precursor to compound **4** must have formed initially and then undergone further reaction with CH$_2$Cl$_2$.

Table 4 Selected internuclear distances (Å) and angles (°) for [Pt(PEt$_3$)$_2${η^5-9-Te(Ph)CH$_2$Cl-7-CB$_{10}$H$_{10}$}] **4** with e.s.d.s in parentheses

Pt–B(3)	2.235(6)	Pt–B(4)	2.244(6)	Pt–B(5)	2.294(6)	Pt–B(2)	2.295(6)
Pt–P(1)	2.3074(14)	Pt–P(2)	2.3189(14)	Pt–C(1)	2.565(5)	Te–C(31)	2.117(6)
Te–C(2)	2.154(7)	Te–B(3)	2.215(6)	C(2)–Cl′	1.67(2)	C(2)–Cl	1.777(8)
C(1)–B(7)	1.670(8)	C(1)–B(5)	1.672(8)	C(1)–B(6)	1.676(8)	C(1)–B(2)	1.686(8)
B(2)–B(8)	1.814(9)	B(2)–B(7)	1.823(8)	B(2)–B(3)	1.839(9)	B(3)–B(8)	1.753(8)
B(3)–B(9)	1.766(8)	B(3)–B(4)	1.782(8)	B(4)–B(10)	1.778(9)	B(4)–B(9)	1.796(9)
B(4)–B(5)	1.895(9)	B(5)–B(10)	1.793(9)	B(5)–B(6)	1.815(8)	B(6)–B(7)	1.753(8)
B(6)–B(11)	1.766(9)	B(6)–B(10)	1.782(9)	B(7)–B(8)	1.784(9)	B(7)–B(11)	1.788(9)
B(8)–B(11)	1.796(9)	B(8)–B(9)	1.799(9)	B(9)–B(11)	1.766(9)	B(9)–B(10)	1.785(9)
B(10)–B(11)	1.805(9)						
B(3)–Pt–B(4)	46.9(2)	B(3)–Pt–B(5)	77.9(2)	B(4)–Pt–B(5)	49.3(2)		
B(3)–Pt–B(2)	47.9(2)	B(4)–Pt–B(2)	79.8(2)	B(5)–Pt–B(2)	72.1(2)		
B(3)–Pt–P(1)	137.5(2)	B(4)–Pt–P(1)	95.6(2)	B(5)–Pt–P(1)	91.5(2)		
B(2)–Pt–P(1)	161.9(2)	B(3)–Pt–P(2)	115.2(2)	B(4)–Pt–P(2)	159.4(2)		
B(5)–Pt–P(2)	146.8(2)	B(2)–Pt–P(2)	93.8(2)	P(1)–Pt–P(2)	96.17(5)		
B(3)–Pt–C(1)	73.8(2)	B(4)–Pt–C(1)	75.7(2)	B(5)–Pt–C(1)	39.8(2)		
B(2)–Pt–C(1)	40.1(2)	P(1)–Pt–C(1)	121.77(12)	P(2)–Pt–C(1)	111.73(12)		
C(31)–Te–C(2)	93.7(3)	C(31)–Te–B(3)	104.2(2)	C(2)–Te–B(3)	101.9(3)		
Cl′–C(2)–Te	118.3(13)	Cl–C(2)–Te	108.7(4)	C(13)–P(1)–C(15)	102.7(3)		
C(13)–P(1)–C(11)	101.6(3)	C(15)–P(1)–C(11)	103.2(3)	C(13)–P(1)–Pt	116.4(2)		
C(15)–P(1)–Pt	116.1(2)	C(11)–P(1)–Pt	114.8(2)	C(23)–P(2)–C(21)	102.9(3)		
C(23)–P(2)–C(25)	101.2(3)	C(21)–P(2)–C(25)	101.4(3)	C(23)–P(2)–Pt	115.6(2)		
C(21)–P(2)–Pt	115.0(2)	C(25)–P(2)–Pt	118.5(2)				

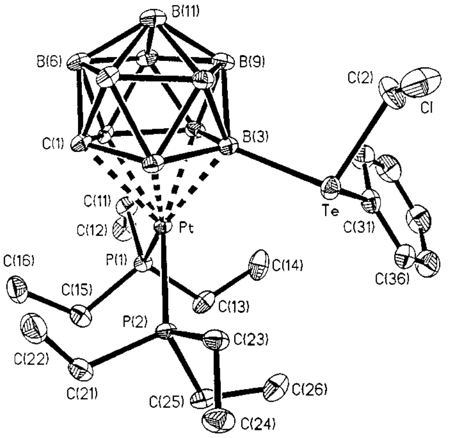

Fig. 5 Molecular structure of [Pt(PEt$_3$)$_2${η^5-9-Te(Ph)CH$_2$Cl-7-CB$_{10}$H$_{10}$}] **4**. Details as in Fig. 1

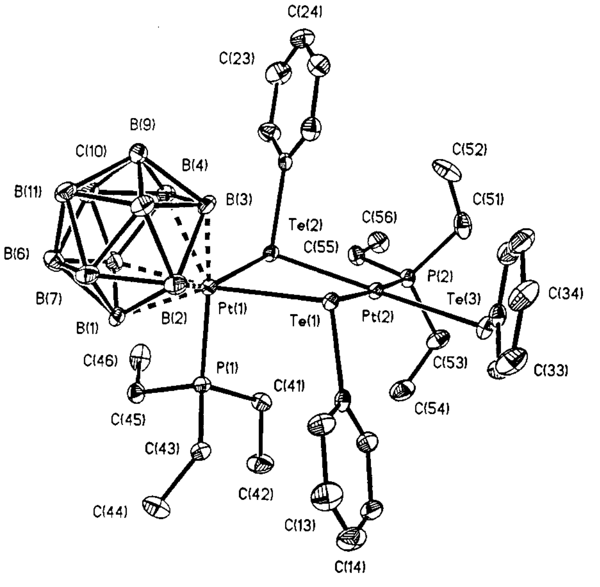

Fig. 6 Molecular structure of [Pt$_2$(TePh)(μ-TePh)$_2$(PEt$_3$)$_2$(η^5-2-CB$_{10}$H$_{11}$)] **5**. Details as in Fig. 1

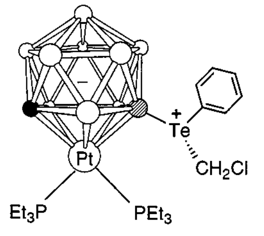

4

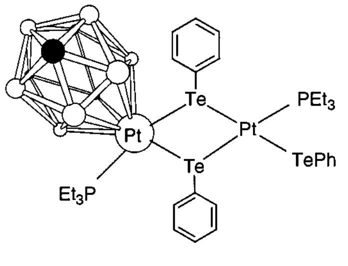

5

○ BH ▨ B ● CH

The ^{31}P-{^{1}H} NMR spectrum (Table 1) of complex **4** shows two resonances in accord with the non-equivalence of the PEt$_3$ ligands. Several peaks in the ^{11}B-{^{1}H} NMR spectrum were broad and overlapped, and little could be inferred from this spectrum. However, a signal corresponding in intensity to a single boron atom at δ −4.7 is assigned to the *B*Te nucleus since in a fully coupled ^{11}B spectrum it remained a singlet. A broad peak in the ^{13}C-{^{1}H} NMR spectrum at δ 50.2 is diagnostic for the cage-carbon atom.

The X-ray diffraction study of the red product **5** established its formulation as the diplatinum complex [Pt$_2$(TePh)(μ-TePh)$_2$(PEt$_3$)$_2$(η^5-2-CB$_{10}$H$_{11}$)]. The molecule is shown in Fig. 6 and important bond distances and angles are given in Table 5. There are several features of interest in the structure. Two TePh groups bridge the Pt(1) and Pt(2) atoms, with Pt(1) carrying PEt$_3$ and η^5-2-CB$_{10}$H$_{11}$ ligands, and Pt(2) a TePh and a PEt$_3$ group. In the bridge system the Pt(1)–Te(1) [2.7220(6) Å] and Pt(1)–Te(2) [2.7054(6) Å] bond lengths are perceptibly longer than the Pt(2)–Te(1) [2.6175(6)] and Pt(2)–Te(2) [2.6113(7) Å]

Table 5 Selected internuclear distances (Å) and angles (°) for $[Pt_2(TePh)(\mu\text{-}TePh)_2(PEt_3)_2(\eta^5\text{-}2\text{-}CB_{10}H_{11})]$ **5** with e.s.d.s in parentheses

Pt(1)–B(5)	2.203(8)	Pt(1)–B(4)	2.226(7)	Pt(1)–B(3)	2.242(7)	Pt(1)–B(1)	2.242(7)
Pt(1)–B(2)	2.246(7)	Pt(1)–P(1)	2.392(2)	Pt(1)–Te(2)	2.7054(6)	Pt(1)–Te(1)	2.7220(6)
Pt(2)–P(2)	2.284(2)	Pt(2)–Te(2)	2.6113(7)	Pt(2)–Te(1)	2.6175(6)	Pt(2)–Te(3)	2.6225(7)
B(1)–B(6)	1.757(10)	B(1)–B(7)	1.782(9)	B(1)–B(2)	1.840(10)	B(1)–B(5)	1.840(10)
B(2)–B(8)	1.787(10)	B(2)–B(7)	1.790(11)	B(2)–B(3)	1.878(10)	B(3)–B(9)	1.774(10)
B(3)–B(8)	1.803(10)	B(3)–B(4)	1.820(11)	B(4)–C(10)	1.693(9)	B(4)–B(9)	1.743(10)
B(4)–B(5)	1.885(10)	B(5)–B(10)	1.718(10)	B(5)–B(6)	1.758(10)	B(6)–C(10)	1.711(10)
B(6)–B(7)	1.767(10)	B(6)–B(11)	1.796(11)	B(7)–B(8)	1.781(11)	B(7)–B(11)	1.785(10)
B(8)–B(11)	1.769(11)	B(8)–B(9)	1.786(11)	B(9)–C(10)	1.688(10)	B(9)–B(11)	1.755(10)
C(10)–B(11)	1.718(10)	Te(1)–C(1)	2.131(6)	Te(2)–C(21)	2.119(6)	Te(3)–C(31)	2.124(6)
B(5)–Pt(1)–Te(2)	105.1(2)	B(4)–Pt(1)–Te(2)	85.5(2)	B(3)–Pt(1)–B(2)	108.7(2)		
B(1)–Pt(1)–Te(2)	150.9(2)	B(2)–Pt(1)–Te(2)	156.3(2)	P(1)–Pt(1)–Te(2)	88.50(4)		
B(5)–Pt(1)–Te(1)	168.4(2)	B(4)–Pt(1)–Te(1)	120.4(2)	B(3)–Pt(1)–Te(1)	83.6(2)		
B(1)–Pt(1)–Te(1)	129.0(2)	B(2)–Pt(1)–Te(1)	88.1(2)	P(1)–Pt(1)–Te(1)	95.66(4)		
Te(2)–Pt(1)–Te(1)	79.24(2)	P(2)–Pt(2)–Te(2)	94.79(4)	P(2)–Pt(2)–Te(1)	176.91(4)		
Te(2)–Pt(2)–Te(1)	82.89(2)	P(2)–Pt(2)–Te(3)	87.60(4)	Te(2)–Pt(2)–Te(3)	177.20(2)		
Te(1)–Pt(2)–Te(3)	94.68(2)	C(11)–Te(1)–Pt(2)	105.4(2)	C(11)–Te(1)–Pt(1)	106.0(2)		
Pt(2)–Te(1)–Pt(2)	97.22(2)	C(21)–Te(2)–Pt(2)	99.7(2)	C(21)–Te(2)–Pt(1)	107.7(2)		
Pt(2)–Te(2)–Pt(1)	97.78(2)	C(31)–Te(3)–Pt(2)	103.7(2)				

bond lengths. This may be the result of the platinum atoms having different formal oxidation states a feature discussed further below in the context of the Pt–P distances. Few platinum–tellurium bond lengths have been recorded but all five bonds in **5** are longer than those found in $[Pt_2Cl_2(\mu\text{-}Cl)(\mu\text{-}TePh)(PBu^n{}_3)_2]$ (2.531 Å)[13] and $[Pt(1,2\text{-}Te_2C_6H_4)(PPh_3)_2]$ (2.589 Å).[14] The phenyl groups attached to Te(1) and Te(2) lie, respectively, below and above the Pt_2Te_2 ring (Fig. 6), the atoms of which are slightly buckled about the Te(1)···Te(2) vector. The dihedral angle between the Pt(1)Te(1)Te(2) and Pt(2)Te(1)Te(2) planes is 163°.

The μ-Te(2)Ph moiety lies *trans* to the Te(3)Ph ligand [Te(2)–Pt(2)–Te(3) 177.20(2)°, Pt(2)–Te(3) 2.6225(7) Å] and μ-Te(1)Ph is *trans* to the $P(2)Et_3$ group [Te(1)–Pt(2)–P(2) 176.91(4)°, Pt(2)–P(2) 2.284(2) Å]. Thus Pt(2) lies in a well defined square planar configuration with respect to its ligands as is normal for Pt^{II}. The maximum deviation of any of the ligated atoms from the mean plane Pt(2)Te(1)Te(2)Te(3)P(2) is only 0.014 Å. The Pt(1) atom carries a PEt_3 group [Pt(1)–P(1) 2.392(2) Å] and is also ligated by a *nido*-$CB_{10}H_{11}$ cage framework. However, unusually the carbon atom in the cage has migrated to the upper pentagonal belt so that Pt(1) is co-ordinated by an open $\overline{\text{BBBBB}}$ face. The X-ray diffraction data for complex **5** were of good quality and collected at low temperatures. This allowed the location of C(10) by comparison of the anisotropic thermal parameters of this atom with its neighbouring atoms. Further confirmation of the correct identification of C(10) comes from an examination of the C(10)–B separations (average 1.70 Å) which as expected for the more electronegative C atom are *ca.* 0.08 Å shorter than related B–B connectivities (1.78 Å) in the boron cage. Migration of carbon atoms in reactions of dicarbon icosahedral metallacarbaboranes containing *nido*-7,8-R_2-7,8-$C_2B_9H_9$ (R = H or Me) ligands is not uncommon,[8,15,16] but a carbon atom site exchange has not to our knowledge been previously observed with a monocarbon icosahedral metallacarbaborane.

The atom Pt(2) is formally Pt^{II}, d^8 with $16e^-$ in its valence shell, counting $2e^-$ each from the terminal $[TePh]^-$ and PEt_3 groups, and four from the μ-TePh system. In contrast Pt(1) is formally Pt^{IV}, d^6 with an $18e^-$ shell receiving $6e^-$ from the $[\textit{nido}\text{-}2\text{-}CB_{10}H_{11}]^{3-}$ anion, 2 from the $P(1)Et_3$ ligand and 4 from the μ-$(TePh)_2$ system. Whereas Pt(2) is ligated by four ligands, the groups around Pt(1) occupy six sites since an η^5 carbaborane cage is generally regarded as being tridentate.[17] In accord with the different co-ordination numbers of the two Pt atoms, the Pt(1)–P(1) bond [2.392(2) Å] is somewhat longer than the Pt(2)–P(2) [2.284(2) Å] connectivity, as is generally found with $PtPEt_3$ complexes with co-ordination numbers of 6 and 4.[5]

The NMR data (Table 1) for compound **5** are in accord with the results of the X-ray diffraction study. In the $^{31}P\text{-}\{^1H\}$ NMR spectrum as expected there are two resonances for the non-equivalent PEt_3 groups. The $^{13}C\text{-}\{^1H\}$ NMR spectrum had a very broad peak at δ 45.5 due to the cage carbon nucleus, and correspondingly there is a singlet peak for this group in the ^1H NMR spectrum at δ 2.66.[8] The $^{11}B\text{-}\{^1H\}$ NMR spectrum revealed broad unresolved peaks affording no diagnostic information.

Conclusion

The motivation for the research described in this paper was to synthesize complexes of the type $[Pt(EPh)(PEt_3)_2(\eta^5\text{-}7\text{-}CB_{10}H_{11})]$ (E = Se or Te) and to investigate their chemistry. Instead several new compounds were obtained having unprecedented molecular structures. Further studies in this area are warranted, particularly as the pathways by which the various products are formed are uncertain. The structures of **4** and **5** are especially novel, that of the latter arising from a low energy polytopal rearrangement of the cage in the precursor **1**, such a process not having been observed previously in a monocarbon metallacarbaborane.

Experimental

General

All experiments were conducted under an atmosphere of dry argon using Schlenk tube techniques. Solvents were freshly distilled under nitrogen from appropriate drying agents before use. Light petroleum refers to that fraction of boiling point 40–60 °C. Chromatography columns (*ca.* 30 cm long and 3 cm in diameter) were packed under nitrogen with silica gel (Acros 70–230 mesh). The NMR measurements were recorded at the following frequencies: ^1H at 360.13, ^{13}C at 90.56, ^{11}B at 115.55 and ^{31}P at 145.78 MHz. The reagents *nido*-7-NMe_3-7-$CB_{10}H_{12}$[18] and $[PtCl_2(PEt_3)_2]$[19] were prepared according to literature methods. The salt $Na_3[\textit{nido}\text{-}7\text{-}CB_{10}H_{11}]$ was synthesized according to the method of Knoth *et al.*[20] and used to prepare $Na[Pt(PEt_3)_2(\eta^5\text{-}7\text{-}CB_{10}H_{11})]$ **1** as described earlier.[1a] The species Te_2Ph_2, PhSeCl and Se_2Ph_2 were used as commercially supplied by Aldrich.

Synthesis of the platinum–selenium complexes

A thf (20 cm^3) solution of the reagent **1** (0.50 mmol), prepared *in situ* and cooled with a toluene–liquid nitrogen bath to −95 °C, was added to a thf (10 cm^3) solution of PhSeCl (0.25 g, 0.50 mmol) using a syringe. After warming the mixture to room

Table 6 Crystallographic data and refinement details for compounds **2a**–**5**

	2a	**3**	**4**	**5**
Formula	$C_{19}H_{35}B_{10}PPtSe_2$	$C_{17}H_{38}B_{10}ClOPPtSe$	$C_{20}H_{47}B_{10}ClP_2PtTe{\cdot}CH_2Cl_2$	Monoclinic
M	755.6	707.04	900.68	$P2_1/c$
Colour, habit	Purple prism	Orange block	Yellow block	22.050(5)
Crystal size/mm	0.30 × 0.40 × 0.60	0.10 × 0.20 × 0.30	0.50 × 0.40 × 0.20	10.023(2)
Crystal system	Monoclinic	Monoclinic	Monoclinic	21.422(4)
Space group	$P2_1/n$	$P2_1/c$	$P2_1/c$	115.40(2)
a/Å	9.139(3)	11.2452(11)	17.617(2)	4276.7(14)
b/Å	14.9839(11)	11.9971(13)	10.8358(8)	4
c/Å	20.095(3)	20.475(3)	17.866(2)	2.131
β/°	98.85(2)	99.035(13)	97.036(11)	86.38
U/Å^3	2772.6(9)	2728.0(6)	3384.8(6)	2536
Z	4	4	4	5–50
D_c/g cm^{-3}	1.810	1.722	1.767	19 603
μ(Mo-Kα)/cm^{-1}	77.52	66.45	53.36	7479
F(000)	1440	1368	1744	0.0398
2θ Range/°	5–50	4–50	5–50	−21 to 26, −11 to
Reflections collected	12 953	14 147	17 692	11, −25 to 25
Unique reflections	4858	4814	5932	0.0715
R(int)	0.0413	0.0261	0.0307	(0.0295)
h,k,l Ranges	−11 to 9, −17 to 17, −23 to 16	−13 to 14, −15 to 11, −26 to 24	−20 to 20, −12 to 12, −8 to 21	0.0248, 17.5048 1.35, −1.18
Final residuals* $wR2$	0.0953	0.0787	0.0819	
($R1$)	(0.0394)	(0.0308)	(0.0298)	
Weighting factors* a, b	0.0498, 0.0000	0.0447, 2.6472	0.0343, 23.1239	1.171
Final electron-density difference features (maximum,minimum)/e Å^{-3}	2.07, −1.30	2.899, −1.421	0.89, −1.11	
Goodness of fit on F^2	1.009	1.061	1.095	

* Refinement was by full-matrix least squares on all F^2 data: $wR2 = [\Sigma w(F_o^2 - F_c^2)^2/\Sigma w(F_o^2)^2]^{\frac{1}{2}}$ where $w = [\sigma^2(F_o^2) + (aP)^2 + bP]^{-1}$ and $P = [\max(F_o^2, 0) + 2F_c^2]/3$. The value in parentheses is given for comparison with refinements based on F_o with a typical threshold of $F \geqslant 4\sigma(F)$ with $R1 = \Sigma||F_o| - |F_c||/\Sigma|F_o|$ and $w^{-1} = [\sigma^2(F_o) + g|F_o|^2]$.

temperature it was stirred for 2 h. Solvent was removed *in vacuo* and the dark yellow residue was dissolved in CH_2Cl_2 (50 cm^3) and filtered through a Whatman 1 µm poly(tetrafluoroethylene) membrane. The volume of the filtrate was reduced to *ca.* 5 cm^3 and loaded onto a silica gel column. Elution with CH_2Cl_2–light petroleum (1 : 3) afforded a blue-purple band **2b**, followed quickly by an intense red-purple band **2a** and then a deep red band **3**. Further elution with CH_2Cl_2–light petroleum (1 : 1) afforded a yellow fraction containing $[Pt(SePh)_2(PEt_3)_2]$. Solvent was removed *in vacuo* from each eluate and the respective solids obtained crystallized. In this manner purple prisms of $[Pt(SePh)(PEt_3)(\eta^5\text{-8-SePh-7-CB}_{10}H_{10})]$ **2a** (0.030 g, 15%) (Found: C, 30.2; H, 4.7. $C_{19}H_{35}B_{10}PPtSe_2$ requires C, 30.2; H, 4.7%) were obtained from pentane at −60 °C, and bluish purple *microcrystals* of $[Pt(SePh)(PEt_3)(\eta^5\text{-9-SePh-7-CB}_{10}H_{10})]$ **2b** (0.015 g, 8%) (Found: C, 30.4; H, 4.8. $C_{19}H_{35}B_{10}PPtSe_2$ requires C, 30.2; H, 4.7%) were obtained from CH_2Cl_2–pentane (1 : 8, 2 cm^3). Red crystals of $[Pt(SePh)(PEt_3)\{\eta^5\text{-8-O}(CH_2)_4\text{Cl-7-CB}_{10}H_{10}\}]$ **3** (0.07 g, 35%) (Found: C, 28.9; H, 5.4. $C_{17}H_{38}B_{10}ClOPPtSe$ requires C, 29.9; H, 5.4%) were grown by diffusion of a hexane solution of the complex into CH_2Cl_2. Finally yellow crystals of $[Pt(SePh)_2(PEt_3)_2]$ (0.03 g, 15%) (Found: C, 39.0; H, 5.4. $C_{24}H_{40}P_2PtSe_2$ requires C, 39.0; H, 5.4%) were isolated from CH_2Cl_2–hexane (1 : 4, 5 cm^3).

If Ph_2Se_2 was the reagent of choice the isomers **2** were formed but **3** was not observed.

Synthesis of the platinum–tellurium complexes

A freshly prepared thf (20 cm^3) solution of complex **1** (0.66 mmol), prepared *in situ*, was cooled to −95 °C, then a thf (15 cm^3) solution containing Te_2Ph_2 (0.135 g, 0.33 mmol) and iodine (0.083 g, 0.33 mmol) (yielding PhTeI) was added using a syringe. After warming to room temperature, an orange-brown solution formed and this was maintained at 40 °C for 1 h. Solvent was removed *in vacuo*, the residue extracted with CH_2Cl_2 (20 cm^3) and filtered through a Whatman 1 µm poly(tetrafluoroethylene) membrane to give a clear deep red solution which was reduced in volume to *ca.* 5 cm^3. Column chromatography, eluting with CH_2Cl_2–light petroleum (3 : 1) removed an orange-red band of **5** followed by a bright yellow band of **4**. Evaporation of solvent *in vacuo* and then crystallization of the respective solids from CH_2Cl_2–light petroleum (1 : 8, 5 cm^3) gave yellow block-like crystals of $[Pt(PEt_3)_2\{\eta^5\text{-9-Te(Ph)CH}_2\text{Cl-7-CB}_{10}H_{10}\}]$ **4** (0.075 g, 20%) (Found: C, 29.8; H, 6.0. $C_{20}H_{47}B_{10}ClP_2PtTe$ requires C, 29.5; H, 5.8%), and deep red prisms of $[Pt_2(TePh)(\mu\text{-TePh})_2(PEt_3)_2(\eta^5\text{-2-CB}_{10}H_{11})]$ **5** (0.085 g, 25%) (Found: C, 27.0; H, 4.0. $C_{31}H_{56}B_{10}P_2Pt_2Te_3$ requires C, 27.1; H, 4.1%).

Crystallography

Crystals of complex **2a** were grown from *n*-hexane by cooling to −60 °C. Crystals of **3**, **4** and **5** were grown by diffusion of *n*-hexane into CH_2Cl_2 solutions of the complexes. Crystals of complex **4** were obtained as large yellow plates and that used for data collection was cut from a larger crystal. All crystals were mounted on glass fibres and data were collected at 173 K on a Siemens SMART CCD area detector three-circle (**2a**, **3** and **4**) or P4 four-circle (**5**) diffractometers (Mo-Kα X-radiation, graphite monochromator, $\bar{\lambda}$ = 0.710 73 Å). It was confirmed that crystal decay had not taken place during the course of the data collections. In the studies of **2a**, **3** and **4**, narrow 'frames' were collected for 0.3° increments in ω for three settings of ϕ. In each of these three cases a total of 1271 frames of data were collected affording rather more than a hemisphere of data for each experiment. The substantial redundancy in data allows empirical absorption corrections (SADABS)[21] to be applied using multiple measurements of equivalent reflections. The data frames were integrated using SAINT.[21] For **5** data were collected with the diffractometer operating in the ω-scan mode using XSCANS.[21] Data were corrected for Lorentz-polarization and X-ray absorption effects, the latter by a semiempirical method based upon ψ-scan data. All structures were solved by conventional direct methods and refined by full-matrix least squares on all F^2 data using SHELXTL version 5.03.[21]

All non-hydrogen atoms were refined with anisotropic thermal parameters. The cage carbon atoms in all complexes were identified by their thermal parameters and bond distances to adjacent boron atoms. All hydrogen atoms were included in calculated positions with isotropic thermal parameters *ca.* 1.2 × (aromatic CH or BH) or 1.5 × (Me) the equivalent isotropic thermal parameters of their parent carbon atoms. The Cl atom of the TeCH$_2$Cl group in compound **4** is disordered over two sites (67 : 33). The thermal parameters for the disordered Cl with major site occupancy are appreciably lower than those of the minor component and therefore the former is shown in Fig. 5. Additionally, the asymmetric unit contains one molecule of CH$_2$Cl$_2$ which is also disordered with two positions for the carbon atom. The molecule of CH$_2$Cl$_2$ lies close to the TeCH$_2$Cl group in the asymmetric unit and it is probable that the disorder observed in these groups is caused by mutual packing interactions. Chemically equivalent distances within the disordered groups were weakly restrained to be equivalent to assist stable refinement. All calculations were carried out on Silicon Graphics Iris, Indigo or Indy computers and experimental data are summarised in Table 6.

CCDC reference number 186/1044.

See http://www.rsc.org/suppdata/dt/1998/2839/ for crystallographic files in .cif format.

Acknowledgements

We thank the Robert A. Welch Foundation for support (Grant AA-1201), Dr. Paul A. Jelliss for many helpful discussions and Dr. Dianne Ellis for the MO calculations.

References

1 (*a*) S. A. Batten, J. C. Jeffery, P. L. Jones, D. F. Mullica, M. D. Rudd, E. L. Sappenfield, F. G. A. Stone and A. Wolf, *Inorg. Chem.*, 1997, **36**, 2570; (*b*) J. C. Jeffery, P. A. Jelliss and F. G. A. Stone, *Organometallics*, 1998, **17**, 1402; (*c*) I. Blandford, J. C. Jeffery, H. Redfearn, L. H. Rees, M. D. Rudd and F. G. A. Stone, *J. Chem. Soc., Dalton Trans.*, 1998, 1669.

2 G. D. Freiser, J. L. Little, J. C. Huffmann and L. J. Todd, *Inorg. Chem.*, 1979, **18**, 755.

3 W. B. Hewer, A. E. True, P. N. Swepson and B. M. Hoffmann, *Inorg. Chem.*, 1988, **27**, 1474 and refs. therein.

4 G. Ferguson, M. Parvez, J. A. McCurtian, O. N. Dhubhghaill, T. R. Spalding and D. Reed, *J. Chem. Soc., Dalton Trans.*, 1987, 699; Faradoon, O. N. Dhubhghaill, T. R. Spalding, G. Ferguson, B. Kaitner, X. L. R. Fontaine and J. D. Kennedy, *J. Chem. Soc., Dalton Trans.*, 1989, 1657.

5 A. G. Orpen, L. Brammer, F. H. Allen, O. Kennard, D. Watson and R. Taylor, *J. Chem. Soc., Dalton Trans.*, 1989, S1.

6 CAChe Scientific, The Oxford Molecular Group, Oxford, 1994.

7 C. A. Tolman, *Chem. Rev.*, 1977, **77**, 313.

8 S. A. Brew and F. G. A. Stone, *Adv. Organomet. Chem.*, 1993, **35**, 135.

9 (*a*) D. F. Mullica, E. L. Sappenfield, F. G. A. Stone and S. F. Woollam, *Organometallics*, 1994, **13**, 157; (*b*) M. Gómez-Saso, D. F. Mullica, E. L. Sappenfield and F. G. A. Stone, *Polyhedron*, 1996, **15**, 793.

10 T. Peymann, K. Kück and D. Gabel, *Inorg. Chem.*, 1997, **36**, 5138.

11 N. Petragnani, L. Torres and K. J. Wynne, *J. Organomet. Chem.*, 1975, **92**, 185.

12 E. H. S. Wong and M. F. Hawthorne, *Inorg. Chem.*, 1978, **17**, 2863; R. E. King, S. B. Miller, C. B. Knobler and M. F. Hawthorne, *Inorg. Chem.*, 1983, **22**, 3548; H. C. Kang, S. S. Lee, C. B. Knobler and M. F. Hawthorne, *Inorg. Chem.*, 1991, **30**, 2024; I. T. Chizhevsky, I. V. Pisareva, P. V. Petrovskii, V. I. Bregadze, A. I. Yanovsky, Yu. T. Struchkov, C. B. Knobler and M. F. Hawthorne, *Inorg. Chem.*, 1993, **22**, 3393.

13 V. K. Jain, S. Kannan and R. Bohra, *Polyhedron*, 1992, **11**, 1551.

14 D. M. Giolando, T. B. Rauchfuss and A. L. Rheingold, *Inorg. Chem.*, 1987, **26**, 1636.

15 M. F. Hawthorne, K. P. Callahan and R. J. Wiersema, *Tetrahedron*, 1974, **30**, 1795; C. B. Knobler, T. B. Marder, E. A. Mizusawa, R. G. Teller, J. A. Long, P. E. Behnken and M. F. Hawthorne, *J. Am. Chem. Soc.*, 1984, **106**, 2990.

16 S. A. Brew, N. Carr, J. C. Jeffery, M. U. Pilotti and F. G. A. Stone, *J. Am. Chem. Soc.*, 1992, **114**, 2203; S. Li and F. G. A. Stone, *Polyhedron*, 1993, **12**, 1689.

17 T. P. Hanusa, *Polyhedron*, 1982, **1**, 663.

18 J. Plešek, T. Jelínek, E. Drdakova, S. Heřmánek and B. Stíbr, *Collect. Czech. Commun.*, 1984, **49**, 1559.

19 G. W. Parshall, *Inorg. Synth.*, 1970, **12**, 26.

20 W. H. Knoth, J. L. Little, J. R. Lawrence, F. R. Scholer and L. J. Todd, *Inorg. Synth.*, 1968, **11**, 33.

21 Bruker X-ray Instruments, Madison, WI, 1995.

Received 18*th May* 1998; *Paper* 8/03702G